Water-alcohol adsorptive separations using metal-organic frameworks and their composites as adsorbents

Tang, Y.; Tanase, S.

DOI
10.1016/j.micromeso.2019.109946

Publication date
2020

Document Version
Final published version

Published in
Microporous and Mesoporous Materials

Microporous and Mesoporous Materials 295 (2020) 109946

Contents lists available at ScienceDirect

Microporous and Mesoporous Materials

journal homepage: http://www.elsevier.com/locate/micromeso

Water-alcohol adsorptive separations using metal-organic frameworks and their composites as adsorbents

Yiwen Tang, Stefania Tanase *

Van't Hoff Institute for Molecular Science, University of Amsterdam, Science Park 904, 1098 XH, Amsterdam, the Netherlands

ARTICLE INFO

Keywords:
Water-alcohol mixtures
Adsorptive separation
MOFs
MOFs-based composite
Designed synthesis

ABSTRACT

This review gives an overview of the synthetic strategies used for designing metal-organic frameworks (MOFs) and MOFs-based composites studied for water-alcohol separation applications. It shows that various organic linkers, including flexible, hydrophobic and zwitterionic ligands have been used for the synthesis of MOFs with flexible frameworks, highly hydrophobic MOFs as well as MOFs with unique electronic distribution in the pores. Due to their specific structural properties, all these materials show different adsorption behavior in the presence of water and alcohols, being able to separate water-alcohol mixtures. Several studies focused on using microporous MOFs to separate water-alcohol mixtures based on the difference in the molecular size of water and alcohols. Combining MOFs with organic polymers into composites is viewed as a viable alternative to tackle some problems that powdered MOFs may cause in industrial applications. The research so far shows that MOFs embedded in polymer matrixes have led to improved efficiency and mixture permeability when comparing with the performance of pristine polymer membranes. Nevertheless, the design of membranes with high permeability, selectivity and stability is difficult due to the swelling of the polymer matrix as well as the difficulties in retaining the matrix integrity while increasing the MOF loading.

1. Introduction

Separating water/alcohol mixtures is one of the most challenging problems associated with the practical application of bioethanol as an environmentally benign and sustainable fuel [1,2]. Bioethanol is currently produced from agricultural feedstocks, algae farms or fermentation of molasses. Thus, it unavoidably contains some impurities such as water and methanol [3,4]. These impurities must be removed to generate fuel-grade ethanol (99.5%). Before entering the engine system, bioethanol must be purified because the impurities reduce the fuel conversion efficiency, and can cause corrosion, reduced lubricity and even microbe growth [5–7]. The traditional distillation approach, widely applied in the chemical industry to separate water-alcohol mixtures, is not effective in generating fuel-grade bio-ethanol from water-alcohol dilute solutions because water and ethanol form an azeotropic mixture [8]. Around *ca.* 4% of the water cannot be removed by distillation from a water-ethanol binary mixture [9,10]. An alternative approach implies the use of separation agents, known as entrainers. The role of the entrainers is to alter the vapor-liquid equilibrium of the water-alcohol mixture in order to reach the complete separation of the two components [11–13]. However, this approach requires high energy costs to recover the entrainers [12,13].

One cost-effective and green alternative to distillation is adsorptive separation [14]. This method uses porous adsorbents to adsorb selectively either water or alcohols. Several porous adsorbents, including zeolites [15], activated carbons [16] and polymers [17] have been used. The efficiency of the separation process depends on the porous structure of the adsorbents that can distinguish between the different molecular size of water and alcohols or the specific interactions between the adsorbent and the constituents of the water-alcohol mixture [8,15–17]. However, the water and alcohol molecules can compete for the adsorption sites, such as in silicate-1, leading to a low separation efficiency [18,19]. In the case of activated carbons, their potential for repeated applications still has to be evaluated [16]. The main drawback of the organic polymers is the so-called plasticization effect, which can cause swelling of the polymer and therefore decreasing the separation efficiency [20]. Due to these limitations, valid alternative porous adsorbents are still needed in the future.

Metal-organic frameworks (MOFs), also known as porous coordination polymers (PCPs), are emerging adsorbent materials constructed

* Corresponding author.
E-mail address: s.grecea@uva.nl (S. Tanase).

https://doi.org/10.1016/j.micromeso.2019.109946
Received 13 August 2019; Received in revised form 5 December 2019; Accepted 6 December 2019
Available online 9 December 2019
1387-1811/

from metal ions or clusters of metal ions linked by organic linkers [21]. Their high surface area as well as the size and the functionality of their pores are key features that determine the uptake capacity and adsorptive selectivity. These features can be greatly influenced by the nature of the metallic nodes and organic linkers. For instance, using long organic linkers in constructing MOFs with a given structure can enlarge the pore size of MOFs without influencing the overall crystal structure [22–24]. Grafting functional groups on the organic linkers through post modification can alter the functionality of MOFs [25]. In principle, constructing MOFs with specific surface area, pore structure and functionality can be reached through the rational design of the organic linkers and the appropriate choice of metal centers [26–29]. Therefore, MOFs are widely used for a variety of applications, including CO_2 capture [30–32], H_2 storage [33], CH_4 storage [34], hydrocarbons separation [35–39] and adsorption-driven heating pumps [40]. However, much fewer studies have focused on the potential application of MOFs in water-alcohol separations.

Utilizing porous adsorbents to separate mixtures into pure components depends mainly on the differences in the chemical properties of the components in a given mixture. Water and alcohols, especially methanol and ethanol, have very similar chemical properties, among which the molecular size and polarity are 2.68 Å/1.0, 3.6 Å/0.76 and 4.5 Å/0.65 for water, methanol and ethanol, respectively [41,70]. Therefore, it is very difficult to distinguish such small differences, even with appropriate pore size and functionality of well-designed MOFs. Water stability of MOFs is another significant property when considering their potential application in water-alcohol separations. For instance, carboxylate-based MOFs usually lack water stability because the metal-carboxylate bond can undergo hydrolysis in the presence of water [42].

This review discusses the strategies used to overcome the main challenges related to the application of MOFs in water-alcohol separations. In the first part, the synthesis approaches used to obtain new MOFs with potential in water-alcohol separations are summarized. The second part focuses on strategies to improve the water-alcohol separation selectivity or water stability of the reported MOFs by combining them with polymers into mixed matrix membranes (MMMs) [20].

2. Synthesis strategies for designing MOFs for water-alcohol separations

2.1. MOFs with flexible organic linkers

Due to the very close values of the kinetic diameter and polarity of the water, methanol and ethanol molecules, it is difficult to design rationally MOFs with appropriate pore size or/and affinity for the separation of these three molecules. MOFs with flexible networks have attracted interest because their flexible structures can undergo rearrangements in response to different specific adsorbate molecules, therefore leading to unconventional adsorption behaviors [43]. Such type of MOFs may also present different adsorption properties in the presence of water and alcohol molecules, hence having potential in the separation of water-alcohol mixtures. The synthesis of the MOFs discussed in this review employs the conventional solvothermal method, dissolving the metal salt and the organic ligand in a solvent or mixture of solvents, followed by subsequent heating of the mixture until MOF crystals are obtained.

MOFs with flexible networks are usually built from transition metal ions and flexible polydentate organic linkers. Two types of flexible ligands, namely tetrakis[4-(carboxyphenyl)-oxamethyl]methane (H_4L) and tetrakis(*m*-pyridyloxymethylene)methane (mtpm), have been selected to synthesize flexible MOFs in view of their freely rotatable -O-CH_2- moieties (see Fig. 1) [44]. $[Zn_4OL_{1.5}]\cdot 4DMA\cdot 10DEF\cdot 10H_2O$ (DMA = Dimethylacetamide, DME = Dimethoxymethane) contains three pairs of half of the L^{4-} ligand which is coordinated to two $Zn_4O(CO_2)_6$ clusters, thus leading to a bipyramidal cage [44]. Each half of L^{4-} ligand has

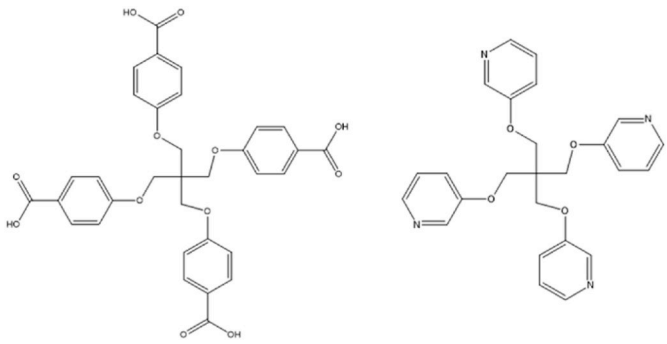

Fig. 1. The structure of H_4L (left) and mtpm (right) linkers.

an angle of 90° due to the rotation of -O-CH_2- moieties. Adjacent cages are further linked through L^{4-} ligands to form a 3D structure which has an intersecting porous system with cross sections of *ca.* 13 Å (Fig. 2) [44]. The oxygen-rich H_4L ligands lead to a porous hydrophilic environment also confirmed by the water, methanol and ethanol adsorption isotherms. The single component adsorption isotherms are of type II, revealing an indefinite multi-layer formation after the monolayer coverage [44]. The pores are large enough for the incorporation of all three molecules. The difference in the uptake at relative saturated pressure, which varies from 12.3 wt% to 5.1 wt%, is likely due to entropic effects. Notably, the water uptake is higher than the methanol and ethanol uptakes, perhaps because the smaller kinetic diameter of water enables it with a more efficient packing in the pores as compared with methanol and ethanol [44,45].

Kitagawa et al. [46,48] used mtpm (Fig. 1) instead of H_4L to synthesize a Cu^{2+}-based flexible MOF because the coordination bonds between pyridyl groups and Cu^{2+} ions are stronger than those between benzoate groups and Cu^{2+} ions, thus increasing the stability of the synthesized MOF (Fig. 2). The MOF obtained, namely $[Cu(mtpm)Cl_2]\cdot 20H_2O$, has a 3D structure built up from chains of vertex-sharing CuO_4Cl_2-octahedra, which are further linked through mtpm linkers. This MOF adsorbs selectively water and methanol at 298 K (Fig. 3) [46]. The water adsorption isotherm indicates that water is adsorbed in the low-pressure range and the uptake increases gradually by increasing the pressure. It reveals a strong affinity of the material for water molecules, likely due to the oxygen rich mtpm ligands which provide a hydrophilic environment. The methanol adsorption isotherm is S-shaped and it reveals a low adsorption below $P/P_0 = 0.5$, then it increases sharply [46]. This phenomenon is known as the *gate-opening effect*. The flexible framework expands from a closed structure to an open one by increasing the pressure [47]. Very interestingly, the ethanol adsorption is negligible even at $P/P_0 = 1$ [46]. No gate-opening effect was observed for ethanol, suggesting that the framework requires more energy to expand in order to adsorb ethanol molecules [46].

Another Zn^{2+}-based MOF was synthesized using the H_4L ligand as linker in combination with a second pillar ligand, namely bpy [11]. The bpy (bpy = 4,4`-bipyridine) ligand was used in an attempt to increase the structural stability of the framework [49]. In this MOF, every two Zn^{2+} ions are coordinated by four L^{4-} ligands in a paddle-wheel fashion. The axial sites of the Zn_2 paddle wheel are occupied by two pillar bipyridine ligands to form a 3D framework (Fig. 4) [50]. The methanol, ethanol, 1-propanol and 2-propanol adsorption isotherms show two steps and an uptake of *ca.* 27, 25.5, 26 and 25 wt% at saturated relative pressure, respectively (Fig. 4) [11]. This unique stepped shape of the adsorption isotherms indicate the commence of the gate-opening effect by increasing the pressure, as a result of the freely rotatable –CH_2-O- moieties of L^{4-} ligand [11]. The adsorption near saturation is mainly influenced by entropic effects, thus the methanol uptake is higher than the propanol uptake which has larger molecular size [11]. Introducing bpy ligands in the framework leads to hydrophobic pores and therefore the water uptake remains negligible even at the saturated relative

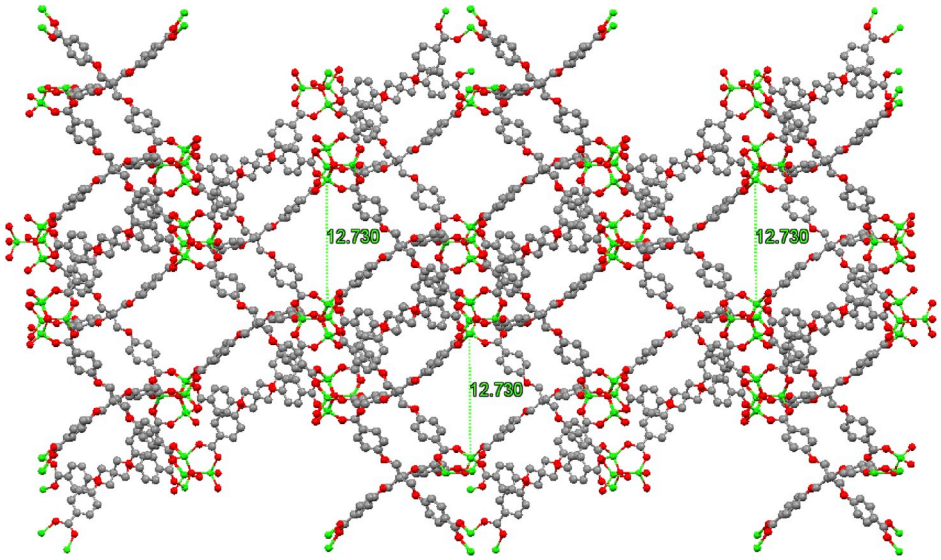

Fig. 2. The 3D structure of $[Zn_4OL_{1.5}]\cdot 4DMA\cdot 10DEF\cdot 10H_2O$ viewed along the *b* axis. All guest molecules are removed for clarity. Color code: Zn, green; C, grey; O, red. (For interpretation of the references to colour in this figure legend, the reader is referred to the Web version of this article.)

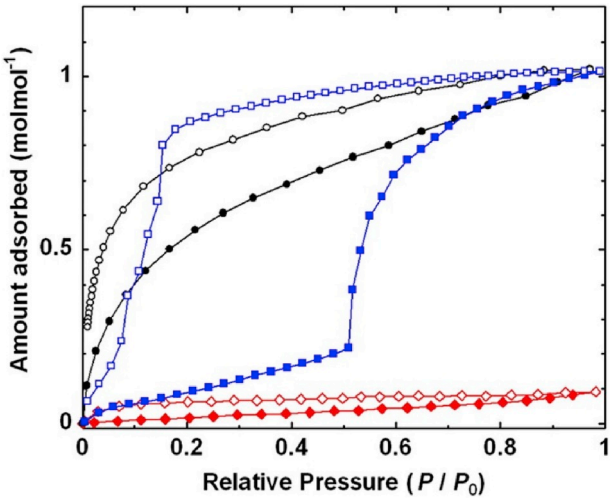

Fig. 3. The water (black), methanol (blue) and ethanol (red) adsorption isotherms of $[Cu(mtpm)Cl_2]\cdot 20H_2O$ measured at 298 K. Closed symbols correspond to adsorption and open symbols correspond to desorption [46]. Reprinted with permission from ref. 46. Copyright (2012) American Chemistry Society. (For interpretation of the references to colour in this figure legend, the reader is referred to the Web version of this article.)

pressure [11].

H_3tci = tri(2-carboxyethyl)-isocyanurate (H_3tci) is an oxygen-rich ligand with three freely rotatable arms, therefore being a good candidate for constructing MOFs with high structural flexibility and hydrophilicity [51]. A Cu^{2+}-based MOF, namely $[Cu_4(OH)_2(tci)_2(bpy)_2]\cdot 11H_2O$, was obtained using tci^{3-} and bpy as linkers, in which bpy was used again to achieve high structural stability [51]. In this MOF, each tetra-nuclear cluster contains six tci^{3-} and four bpy ligands to yield a 3D structure (Fig. 5). The overall topology has an interweaving channel system, with small and big channels of *ca.* 3.4 × 10.6 Å and 11.2 × 12.5 Å respectively. The water, methanol and ethanol adsorption isotherms are of type II and display a hysteresis loop upon desorption. The maximum water, methanol and ethanol uptakes are *ca.* 89, 70 and 73 mg/g at relative saturated pressure ($P/P_0 = 0.9$) and 298 K, respectively [51]. The difference in the adsorption uptakes is mostly due to entropic effects [45]. As for the Cu^{2+}-based flexible MOFs, the water and methanol uptakes are much higher than those of the Cu^{2+}-MOF discussed above [46,51]. For the Cu^{2+}-MOF built from tci^{3-} and bpy, the channels interweave reduce the void space for adsorption, whilst the small pores of *ca.* 5 and 8 Å of the Cu^{2+}-MOF built from mtpm likers prevent the decrease of such adsorption space.

The *gate-opening effect* is associated with the structural flexibility of the MOFs. For the MOFs discussed above, it arises from the flexibility of the organic linkers. This is also the main reason for which these MOFs show different adsorption for water and alcohols. Their frameworks can display different degrees of structural expansion in response to different adsorbate molecules. The surface area and the pore volume of these MOFs have little effect on their water-alcohol separation properties. Only the surface area of $[Cu_4(OH)_2(tci)_2(bpy)_2]\cdot 11H_2O$ is reported and it equals *ca.* 87 m^2/g [51]. Such a small surface area confirms that the structure of $[Cu_4(OH)_2(tci)_2(bpy)_2]\cdot 11H_2O$ undergoes an expansion during water, methanol and ethanol adsorption, therefore the high uptakes obtained.

The *gate-opening effect* is not the only way a flexible MOF can undergo structural rearrangements during adsorption measurements. Another effect called *breathing effect* also reflects the structural rearrangement of flexible MOFs. In this case, the pores of the MOFs can reversibly open and close, with the MOF framework being able to reversible switch between two states corresponding to expansion and contraction, respectively [52]. Thus, a MOF structure presents various porous shapes during the adsorption process. The effect depends strongly on the complex and the competitive nature of the different interactions, including adsorbate-adsorbate and adsorbate-adsorbent interactions, the increasing adsorbate pressure and the flexibility of MOFs' skeleton [52–54].

Cr^{3+}-MIL-53 is a MOF that presents different *breathing effects* during water, methanol and ethanol adsorption processes [55]. The Cr^{3+} ion is coordinated to four oxygen atoms from bdc^{2-} ligands and two oxygen atoms from water molecules to form Cr^{3+} octahedra which are further connected with bdc^{2-} ligands leading to a 3D structure with 1D pores [56]. As shown in Fig. 6, Cr^{3+}-MIL-53 has an empty framework with large pores (LP) before adsorption. During the water adsorption, the LP structure of Cr^{3+}-MIL-53 begins to shrink and gradually transforms into a narrow porous structure (NP) in the range $0.1 < P/P^0 < 0.9$ (Fig. 6). This is because the flexible framework of Cr^{3+}-MIL-53 is dragged by the adsorbed water molecules through hydrogen bonding. A capilary condensation is observed above $P/P^0 = 0.9$ and no re-opening of NP structure can be observed. Because the interactions between

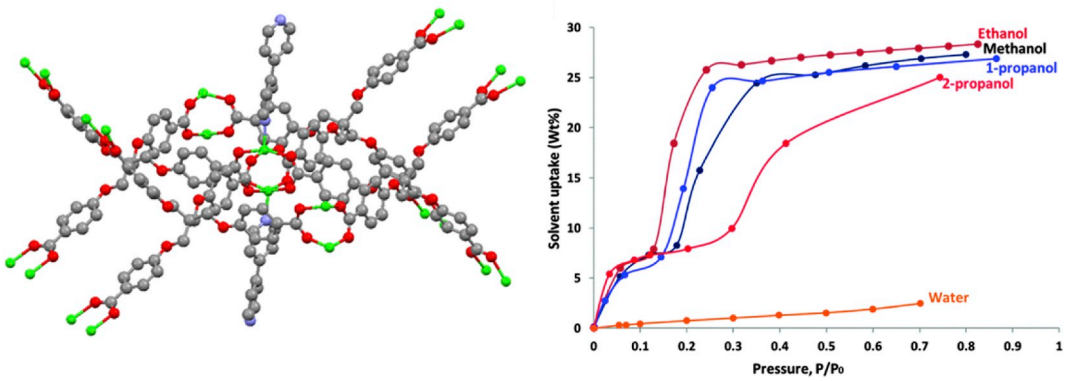

Fig. 4. The Zn_2 paddle-wheel cluster of **TetZB**; (left) and the water, methanol, ethanol, 1-propanol and 2-propanol adsorption isotherms measured at 298 K (right) [11]. Color code: Zn, green; C, grey; O, red; N, purple. The right figure is reprinted with permission from ref. 11. Copyright (2015) Royal Society of Chemistry. (For interpretation of the references to colour in this figure legend, the reader is referred to the Web version of this article.)

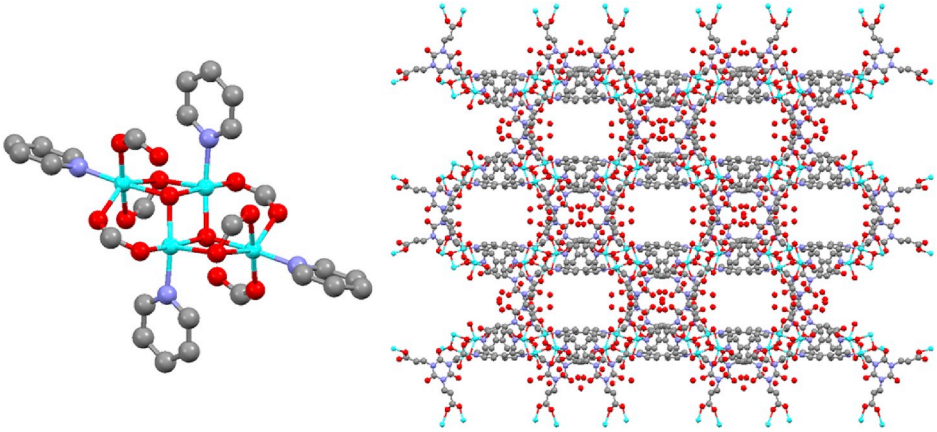

Fig. 5. The tetranuclear copper cluster building unit (left) and the 3D structure (right) of $[Cu_4(OH)_2(tci)_2(bpy)_2]\cdot 11H_2O$. Color code: Cu, blue; C, grey; O, red; N, purple. (For interpretation of the references to colour in this figure legend, the reader is referred to the Web version of this article.)

Cr^{3+}-MIL-53 and adsorbate molecules are stronger for alcohols as compared with water, the shrinkage from LP to NP structure is completed at very low relative pressure. Consequently, no initial plateau can be observed in the alcohol adsorption isotherms (Fig. 6). For both methanol and ethanol adsorption, a reopening from NP back to LP structure is observed when the pressure increases, as reflected by the stepped isotherm above $P/P^0 = 0.1$ (Fig. 6). The difference observed in the structure rearrangement of Cr^{3+}-MIL-53 for water and alcohol adsorption isotherms is due to the adsorbate-adsorbate interactions. For water, a hydrogen-bonding network is formed within the 1D pores of Cr^{3+}-MIL-53, but this is absent in the case of alcohols. The hydrogen bonding interactions contribute to the stabilization of the NP structure, thus hindering the pore reopening to the LP structure [55]. Different than the MOFs showing *gate-opening effect,* for which the surface area seems to have little effect on the adsorption of water and alcohols, the higher surface area of Cr^{3+}-MIL-53 may have influence the uptake of such molecules. The Langmuir surface area of Cr^{3+}-MIL-53 is above 1500 m^2/g after removing all guest molecules at 300 °C [56].

Water stability is one of the most crucial properties of MOFs for determining their potential application in water-alcohol separations. However, none of the studies discussed above focused on this aspect. For instance, there are no reports on the structural stability of MOFs following water adsorption measurements. The lack of water stability testing may hinder the application of water-alcohol separation of these MOFs.

2.2. Hydrophobic MOFs

Alcohol molecules contain both a polar hydroxyl part and a nonpolar alkyl part, therefore their polarity is lower as compared with water. Consequently, highly hydrophobic MOFs are expected to show stronger affinity for alcohols than for water, thus being potential candidates for adsorptive water-alcohol separations. $[Zn_2(bdc)_2(DABCO)]$ (H_2bdc = Benzene-1,4-dicarboxylic acid, DABCO = 1,4-diazabicyclo[2.2.2.]octane) known as DMOF [57,58], ZIF-8,[7,59] and ZIF-71 [59,60] are such examples.

In DMOF, 2D square-grids of $\{Zn_2(bdc)_2\}$ are extended from axial positions by DABCO linkers into a 3D structure [61]. Due to the phenyl and alkyl groups of the bdc^{2-} and DABCO ligands, DMOF is highly hydrophobic, such feature being also confirmed by the water adsorption studies. A negligible water uptake of *ca.* 6 mg/g at $P/P_0 = 0.42$ is observed [57]. The alcohol adsorption uptakes, including methanol and ethanol are much higher, reaching values of *ca.* 520 and 418 mg/g at $P/P_0 = 0.42$, respectively (Fig. 7) [57]. This is because the hydrophobic sites of DMOF, including the phenyl and alkyl parts of the organic ligands, act as adsorption sites for the alkyl groups of the methanol and ethanol molecules [62]. The difference between the methanol and ethanol uptakes were explained in terms of the entropic effects because the smaller methanol molecules are expected to pack more efficiently [57,58].

Although DMOF seems a promising candidate as adsorbent for water-alcohol separations, initial studies did not focus on the water stability of the DMOF [57]. Following studies have demonstrated that DMOF has a

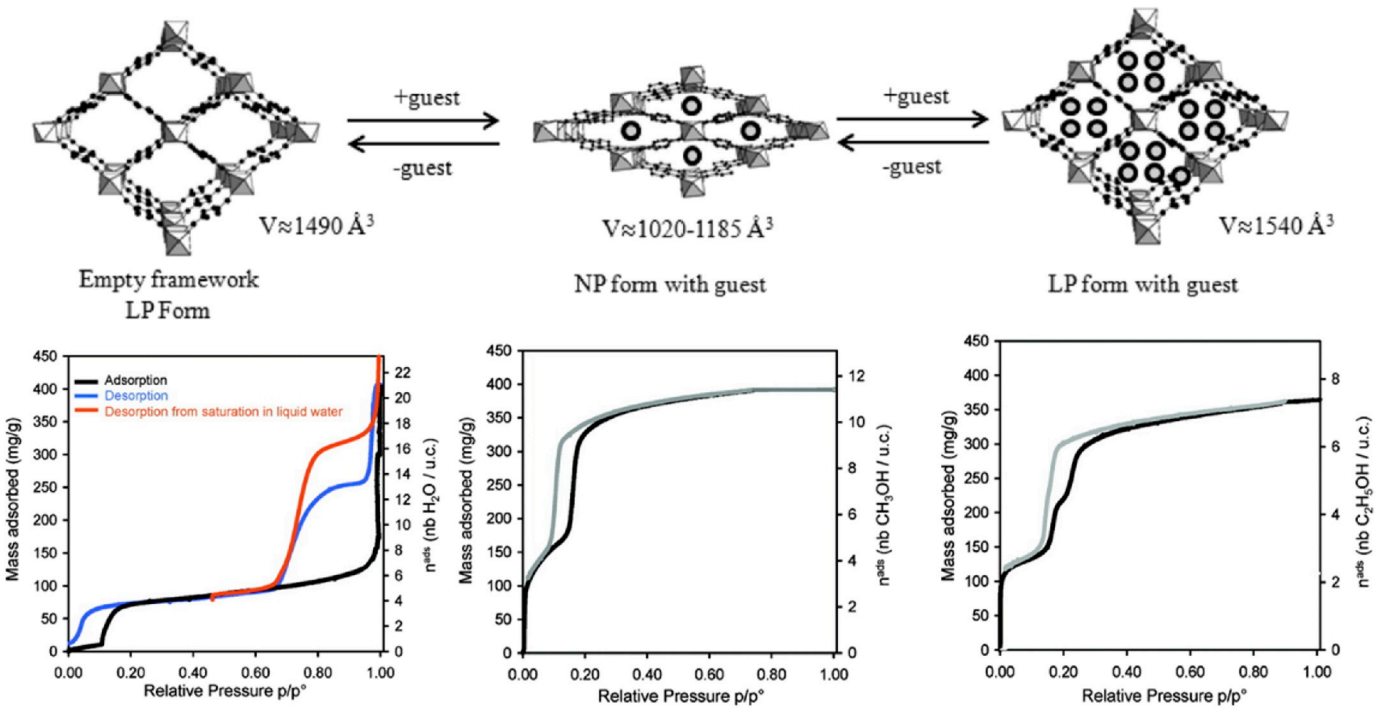

Fig. 6. Top: The structural rearrangement of Cr^{3+}-MIL-53 upon the adsorption of alcohols. Bottom: The water (left), methanol (middle) and ethanol (right) uptake measured 298 K. (left) [55]. Reprinted with permission from ref. 55. Copyright (2010) American Chemistry Society.

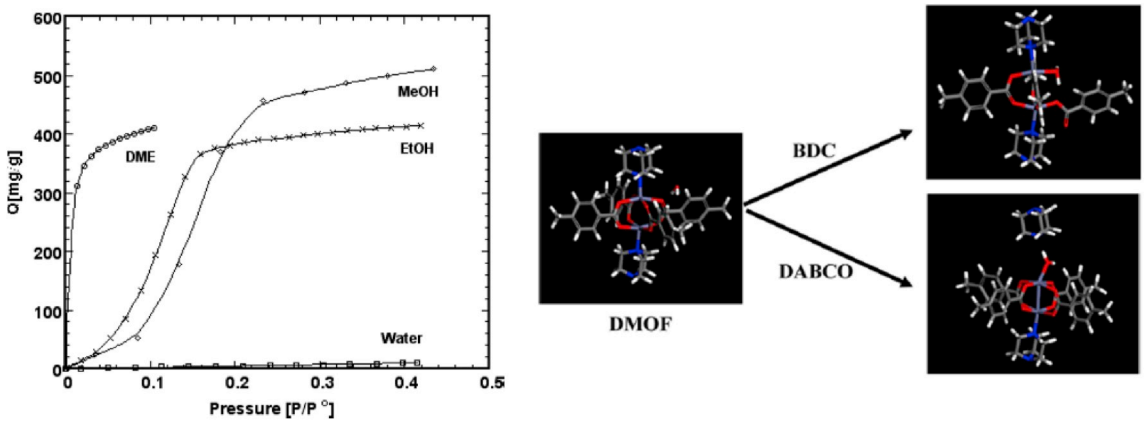

Fig. 7. The dimethylether, methanol, ethanol and water adsorption isotherms of DMOF measured at 298 K (left) [57]. Reprinted with permission from ref. 57. Copyright (2007) Wiley. Schematic illustration of replacing bdc^{2-} and DABCO ligands by water molecules in DMOF (right) [64]. Reprinted with permission from ref. 64. Copyright (2013) American Chemistry Society.

very weak water stability [63,64]. The structure of DMOF undergoes a hydrolysis process above *ca.* 40% relative humidity when the coordinated bdc^{2-} and DABCO ligands are replaced by water molecules, thus leading to the decomposition of the framework (Fig. 7) [63,64]. This weak water stability hinders the application of DMOF in water-alcohol adsorptive separations.

Due to the weak water stability of DMOF, further studies were focused on hydrophobic MOFs with high chemical and thermal stability. The water and alcohol adsorption properties of MOFs were tested on two representatives among the zeolitic imidazolate frameworks (ZIFs), namely ZIF-8 and ZIF-71 [7,59,60,65].

Both ZIF-8 and ZIF-71 are constructed from Zn^{2+} as metal nodes and imidazolate ligands as organic linkers, in which the imidazolate ligands are 2-methylimidazolate (Hmim) and dichloroimidazole (dcIm) for ZIF-8 and ZIF-71, respectively (Fig. 8). The overall hydrophobicity of ZIF-8 and ZIF-71 is confirmed by the type III adsorption isotherm observed for

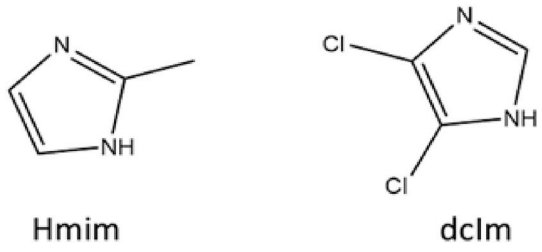

Fig. 8. The structure of Hmim (left) and dcIm (right) linkers.

the water adsorption, corresponding to the weak interaction between their frameworks and water molecules [59]. The water uptake for both ZIF-8 and ZIF-71 is negligible even at the relative saturated pressure. For methanol and ethanol adsorption, both ZIF-8 and ZIF-71 display

S-shaped adsorption isotherms [59]. The methanol and ethanol uptakes are very small in the low pressure range and increase sharply by increasing the pressure [59]. This behavior is generally observed for hydrophobic porous structures which have stronger affinity for alcohols than water. In the low pressure, the alcohol molecules are adsorbed as small clusters which provide interaction sites for the later adsorbed molecules, leading to capillary condensation at higher pressures [7,59,60,66].

The highly hydrophobic structure of DMOF, ZIF-8 and ZIF-71 plays a key role in the preferential adsorption of alcohols and their surface area as well as the pore volume determine their uptake capacity. DMOF has the highest surface area (Brunauer-Emett-Teller (BET) method, 1794 m^2/g) and pore volume (Horvath-Kawazoe (HK) method, 0.65 cm^3/g) among the three MOFs [57]. ZIF-8 and ZIF-71 have BET surface areas of 1696 and 1183 m^2/g as well as a pore volume of 0.63 and 0.39 cm^3/g (*t*-plot method), respectively [59,60]. Therefore, DMOF displays the highest methanol and ethanol uptakes among the three reported MOFs [57,59,60].

Both ZIF-8 and ZIF-71 can selectively adsorb alcohols over water and they also have high chemical and thermal stability, such features recommending them as suitable candidates for practical water-alcohol separation applications. However, the chemical industry prefers that adsorbent materials have favorable alcohol uptakes at low pressure and unfavorable water uptake in the entire pressure region [59]. Therefore, ZIFs adsorbents do not fulfill this requirement because both ZIF-8 and ZIF-71 have unfavorable alcohol uptakes at low pressure. Thus, designing adsorbents with desirable water-alcohol separation properties still remains a big challenge.

2.3. MOFs made using specific synthetic strategies

Some other synthetic strategies for designing MOFs applicable in water-alcohol adsorptive separations focus on utilizing specific interactions between MOFs and adsorbate molecules [67], micro-porous MOFs [68–74], and MOFs with 1D channels and molecular gates, which can only open for specific adsorbate molecules [75,76].

Zhang et al. [67] introduced a zwitterionic bipyridinium ligand (bpybc), to synthesize $[Dy(ox)(bpybc)(H_2O)](OH)\cdot 13H_2O$ (H_2ox = oxalic acid) which has pores featuring a regularly distributed electrostatic field: one side has positive charges whilst the other side has negative charges (Fig. 9). Such feature can contribute to the build-up of coulombic fields in a pore space which can be used for the polarization and polarized binding of polar molecules [67]. Adsorption studies show that the MOF adsorbs water selectively over methanol and ethanol as well as methanol over ethanol (Fig. 9). This adsorption selectivity sequence matches the order of polarity of water, methanol and ethanol from high to low [67]. Similar to the flexible MOFs discussed in section 2.1, the surface area and pore volume of $[Dy(ox)(bpybc)(H_2O)](OH)\cdot 13H_2O$ have little effect on its water-alcohol separation properties [67].

Even though the difference in the molecular size of water, methanol and ethanol is very small, significant research is still devoted to the design of size-selective microporous MOFs for the separation of water-alcohol mixtures [68–74]. The ligands used for the synthesis of such microporous MOFs are shown in Fig. 10 [68–74].

$[Cu(R\text{-}GLA\text{-}Me)(bpy)_{0.5}]\cdot 0.55H_2O$ (R-GLA-Me = R-2-methyl-glutarate) has 1D pores with size of about 2.8 × 3.6 $Å^2$. Such pore is larger than the kinetic diameter of water but comparable to the kinetic diameter of methanol, therefore leading to a higher water uptake (*ca.* 5.1 mmol/g) as compared with methanol (*ca.* 2.1 mmol/g) at 298 K and P/P_0 = 0.96 [68]. Li et al. [69] synthesized $[Co_3(HCOO)_6]\cdot DMF$ (HCOOH = formic acid) which has 1D pores with zigzag shape and size of about *ca.* 5–6 Å. The small pore size observed for this MOF was explained in terms of the strong coordinative bonds between formate and cobalt ions. The zigzag shape of 1D pores in $[Co_3(HCOO)_6]\cdot DMF$ plays an important role in the adsorption of alcohols. It is observed that the steric constrains effect is stronger as the alcohol molecule is larger. Consequently, the value of adsorbed molecules per cell decreased from *ca.* 5.5 for methanol (kinetic diameter of 3.6 Å) to *ca.* 4 for 1-butanol (kinetic diameter above 8 Å) [69]. $[Cd(Hthipc)_2]\cdot 6H_2O$ (H_2thipc = (S)-4,5,6,7-tetrahydro-1*H*-imidazo[4,5-c]pyridine-6-carboxylate), also known as JUC-110 has a square grid framework with 1D hydrophilic pores with size of about 4.5 × 4.5 $Å^2$ [70]. JUC-110 adsorbs water and methanol selectively over ethanol. The water and methanol uptakes are *ca.* 126.7 and 43 cm^3/g, respectively at P/P_0 = 0.95 whilst ethanol uptake is almost negligible, only *ca.* 3.6 cm^3/g at P/P_0 = 0.95. These results indicate that JUC-110 is suitable for size-driven separations of water-alcohol mixtures [70].

Li et al. [71,72] studied the adsorption of water and alcohols using two MOFs having microporous structures. $[Zn(HPyImDC)(DMA)]_n$ ($H_3PyImDC$ = 2-(pyridine-4-yl)-1*H*-4,5-imidazoledicarboxylic acid) has rhombic 1D pores with size of *ca.* 4.8 × 4.0 $Å^2$ [71]. The water, methanol, ethanol, *n*-propanol and *i*-propanol uptakes are *ca.* 95, 60, 23, 16 and 2.6 cm^3/g, respectively at relative saturated pressure (P/P_0 = 0.98). These values vary inversely with the size of the alcohol molecules. [Cd(X)(DMF)] (H_2X = 5-(4-pyridyl)-isophthalic acid) displays microporous windows with size of *ca.* 6.0 × 4.0 $Å^2$ [72]. The water, methanol, ethanol

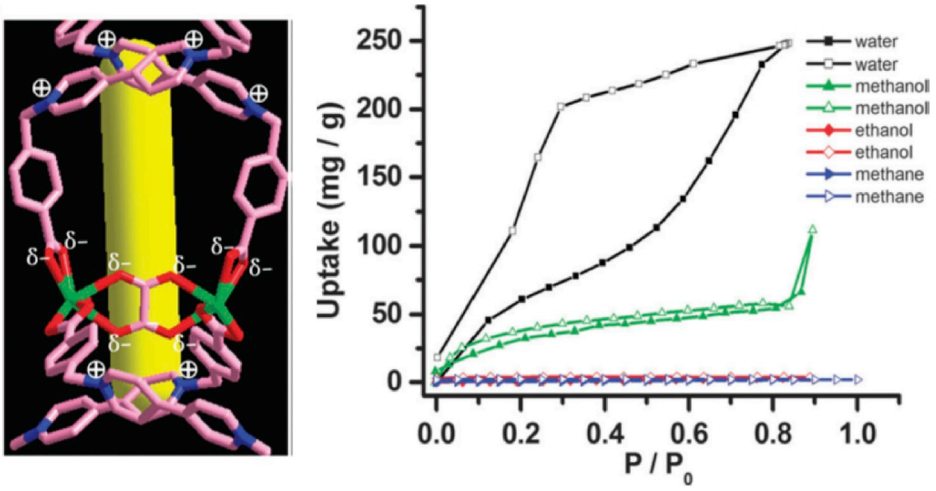

Fig. 9. Schematic representation of the regular charge distribution in the pore of $[Dy(ox)(bpybc)(H_2O)](OH)\cdot 13H_2O$ (left) and its water, methanol and ethanol adsorption isotherms measured at 298 K (right). Closed symbols correspond to adsorption and open symbols correspond to desorption [67]. Reprinted with permission from ref. 67. Copyright (2013) Royal Chemistry Society.

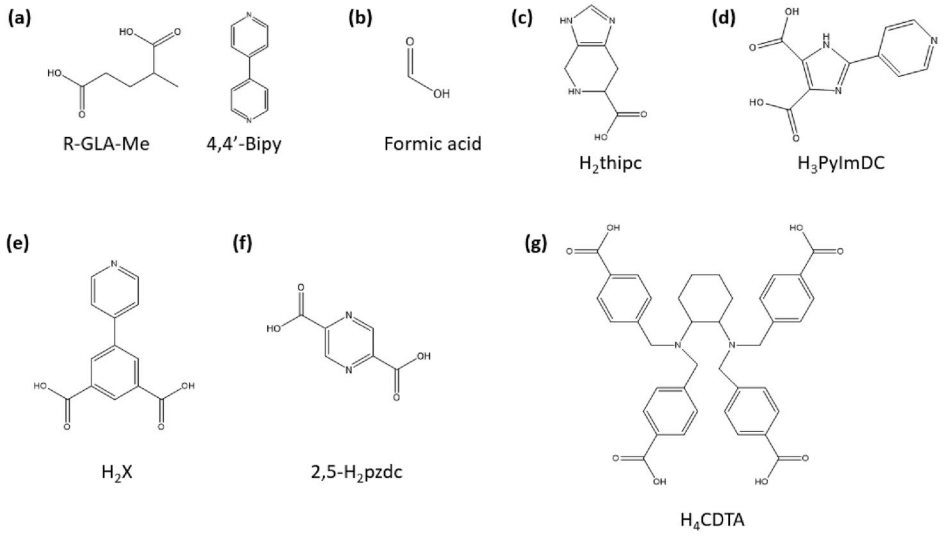

Fig. 10. Organic linkers used for the synthesis of microporous MOFs typically studied for water-alcohol separations.

and *i*-propanol uptakes are *ca.* 188, 74, 38 and 10 cm^3/g, respectively, values decreasing with the increasing size of the adsorbate molecules. Both examples reveal the key role played by the microporous structures in the separation of water and alcohols.

Tanase et al. [73] synthesized a microporous lanthanide-based MOF, $[La(2,5\text{-pzdc})_{1.5}(H_2O)_2]\cdot 2H_2O$ (2,5-H_2pzdc = pyrazine-2,3-dicarboxylic acid) with high selective water adsorption as compared with methanol. The MOF features a 3D structure with hydrophilic 1D tetragonal pores of *ca.* 3.8 × 3.5 $Å^2$ [73]. Such small pores enable only the accessibility of water molecules. Indeed, the water and methanol adsorption studies show that the uptakes are *ca.* 1.2 mmol/g and below 0.1 mmol/g for water and methanol, respectively [73]. Another key feature of $[La(2,5\text{-pzdc})_{1.5}(H_2O)_2]\cdot 2H_2O$ is its impressive water stability, with the structural integrity retained after three consecutive water adsorption cycles [73]. It is also the only microporous MOF discussed here that undergoes a water stability test. The separation efficiency of this material was further supported by the transient breakthrough simulation. The transient breakthrough curve displays the concentration of the single component of mixture in the effluent leaving the packed bed adsorber packed with adsorbent (Fig. 11).

Micropores formation may also result from the interpenetration of highly porous frameworks. For example, $[(NiY)_4(CDTA)_2]\cdot 2.5CH_3CN\cdot 22H_2O$ (H_4CDTA = 4,4′,4″,4‴-(cyclohexane-1,2-diylbis(azanetriyl))tetrakis(methylene)tetrabenzoic acid) is built up from a macrocyclic nickel cluster $[NiY]^{2+}$ and a semirigid linker [74]. It has a fourfold interpenetrated framework (Fig. 12) with 1D pores having a size of about 6 × 8 $Å^2$ [74]. This MOF shows a selective adsorption for methanol and ethanol over *n*-propanol and isopropanol (Fig. 12) [74].

For the MOFs discussed above, the size of the micropores is the key parameter which influences the adsorption of water and alcohol molecules and their surface area and the pore volume correlate well with the adsorbate uptake. The surface area of $[Co_3(HCOO)_6]\cdot$DMF, [Zn(HPyImDC)(DMA)] and [Cd(X)(DMF)] is *ca.* 305, 185 and 230 m^2/g, respectively [69,71,72]. Their corresponding methanol and ethanol uptakes are *ca.* 100/105 mg/g, 85.7/47.2 mg/g and 105.6/78.0 mg/g, respectively [69,71,72]. Indeed, $[Co_3(HCOO)_6]\cdot$DMF has the highest BET surface area as well as the highest methanol and ethanol uptakes.

It is reported that JUC-110,[70] [Zn(HPyImDC)(DMA)] [71], [Cd(X)(DMF)] [72] and $[La(2,5\text{-pzdc})_{1.5}(H_2O)_2]\cdot 2H_2O$ [73] have an excellent water stability. Upon hydrothermal treatment, JUC-110[70] retains its crystallinity for 10 days whilst $[La(2,5\text{-pzdc})_{1.5}(H_2O)_2]\cdot 2H_2O$ keeps it for 72 h [73]. Both [Zn(HPyImDC)(DMA)] and [Cd(X)(DMF)] are stable at ambient conditions for several months [71,72]. In this case, it is proposed that the strong coordinative bonds and the hydrophobic pore structure contribute to superior water stability [70–73,75]. It is reported that several factors influence the water stability of MOFs [75,76,90], including the strength of the covalent coordinative bonds, the stability of the metal clusters in the presence of water, the hydrophobic nature of the MOF as well as steric factors [76]. Several strategies have been proposed to increase the water stability of MOF materials: *(i)* using ligands with high pK_a values to increase the strength of covalent coordinative bonds [75,76]; *(ii)* choosing metal ions with high oxidation state, such as Ti^{4+}, Zr^{4+} and Hf^{4+}, because their high charge density can polarize the oxygen atom of the carboxylate groups to form stronger

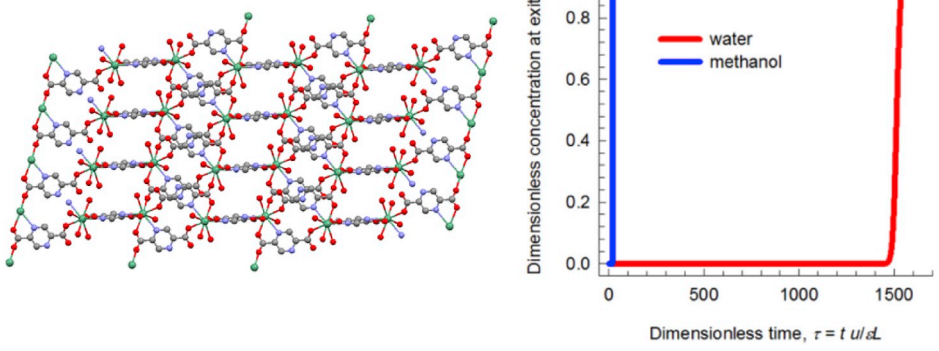

Fig. 11. View of the molecular structure of $[La(2,5\text{-pzdc})_{1.5}(H_2O)_2]\cdot 2H_2O$ showing the tetragonal channels (left) and the breakthrough simulation for a feed vapor mixture of water-methanol (5% of water and 95% of methanol) with total pressure of 100 kPa (right) [73]. Color code: La, olive; C, grey; O, red; N, purple. The right figure is reprinted with permission from ref. 73. Copyright (2014) Wiley. (For interpretation of the references to colour in this figure legend, the reader is referred to the Web version of this article.)

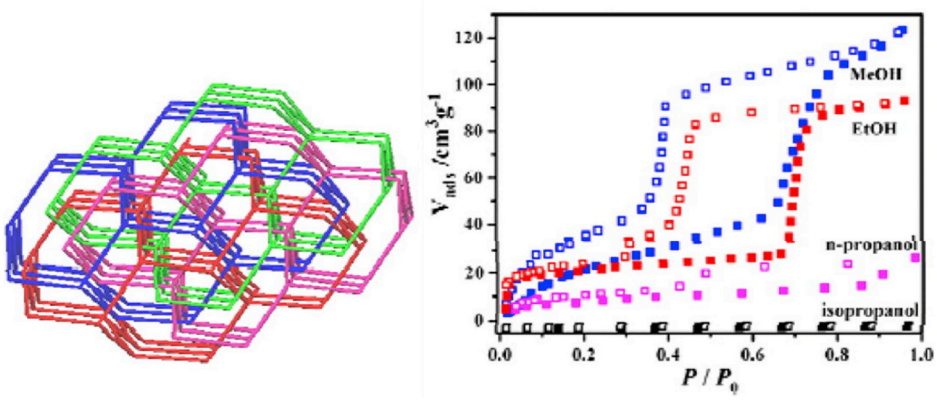

Fig. 12. The fourfold interpenetrating diamondoid frameworks of $[(NiY)_4(CDTA)_2]\cdot 2.5CH_3CN\cdot 22H_2O$ (left) and the methanol, ethanol, *n*-propanol and isopropanol adsorption isotherms measured at 298 K (right) [74]. Closed symbols correspond to adsorption and open symbols correspond to desorption. Reprinted with permission from ref. 74. Copyright (2015) American Chemistry Society.

metal-ligand bonds [75]; *(iii)* incorporating hydrophobic functional groups on the organic linker [76,90]; and *(iv)* blocking the metal centers through steric hindrance to prevent the access of the water molecules [75,76].

The functionality as well as the flexibility of the substituted groups of the organic linkers can also be used to control the adsorption of small organic molecules [77]. Ling et al. [77] synthesized three MOFs by using derivatives of 5-hydroxy-1,3-dicarboxylate benzoic acid (Fig. 13). The functional groups of the linker have a high flexibility degree which varies in the order of $H_2L1<H_2L2<H_2L3$. The propyl group has the highest flexibility due to the largest number of rotatable σ bonds. Adsorption studies showed that the water, methanol and ethanol uptake increased by increasing the flexibility of the additional functional groups (Fig. 13) [77].

It was shown that the adsorption properties of $[Cu_2(tpt)_2(CH_3CN)_2](BF_4)_2$ (H_2tpt = 2,4,6-tri(4-pyridyl)-1,3,5-triazine) can be tuned by incorporating specific anions in its 1D pores [78]. BF_4^- anions are located in the vicinity of Cu^{2+} ions but they occupy the 1D pores. Adsorption studies show that molecular gates can open or close in response to different adsorbent molecules, driven by specific interactions established between BF_4^- anions and the adsorbed molecules [78]. Strong interactions between BF_4^- anions and water or small alcohol molecules (methanol and ethanol) lead to the opening of 1D pores, facilitating the adsorption of these molecules (Fig. 14). For larger alcohol molecules, such as propanol and butanol, the molecular gates remain closed because their size is too large to fit within the 1D channels, therefore $[Cu_2(tpt)_2(CH_3CN)_2]\cdot(BF_4)_2$ adsorbs selectively water and small alcohols [78]. The surface area and the pore volume of Cu-L1, Cu-L2, Cu-L3 and $[Cu_2(tpt)_2(CH_3CN)_2]\cdot(BF_4)_2$ have negligible effect on their adsorption properties [77,78].

3. Mixed matrix membranes containing MOFs

Although some MOFs have demonstrated potential for water-alcohol adsorptive separations, they may not be directly used in industrial applications in the form of powders. Due to their limited packing densities and high diffusion barriers, they may increase the risk of decreasing separation efficiency as well as the contamination or blocking of industrial pipelines [79]. Combing powder MOFs with other materials to form composites is an alternative to overcome this problem. As for water-alcohol separation processes, incorporating MOFs as fillers in polymer matrixes to form mixed matrix membranes (MMMs) is the most used approach [20].

Polymer membranes are commonly used in pervaporation processes in industry. During the pervaporation process, the components of a mixture are adsorbed on one side of the membrane and then evaporated as permeates on the other side [20]. The separation of a mixture is achieved by the differences in the adsorption and diffusion of mixture components [20]. However, the separation efficiency of a mixture using polymer membranes decreases whilst the swelling of polymers occurs, being caused by the plasticization effect [20]. This drawback can be overcome by incorporating inorganic fillers into polymer membranes. MOFs are a promising choice to be used as fillers because they contain organic ligands which are compatible with the polymers. Therefore, combining MOFs with organic polymers into mixed matrix membranes (MMMs) is foreseen to advance the efficiency of water-alcohol separation processes.

The separation efficiency of a MMM is characterized by two key elements, the permeation flux and the separation factor, reflecting the mixture diffusion and the selective adsorption of MMMs. Using MMMs in pervaporation processes aims at removing minor components from a liquid mixture. Consequently, most of the studies focus on removing

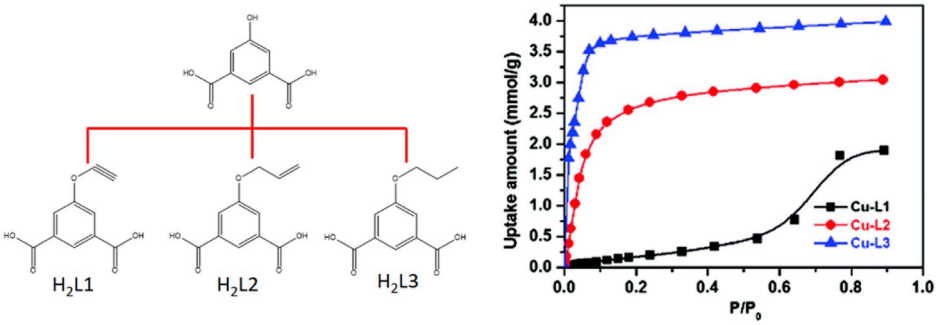

Fig. 13. The organic ligands used for the synthesis of Cu-L1 (H_2L1), Cu-L2 (H_2L2) and Cu-L3 (H_2L3), respectively (left) and the methanol adsorption isotherms of the three MOFs (right) [77]. The right figure is reprinted with permission from ref. 77. Copyright (2016) Royal Chemistry Society.

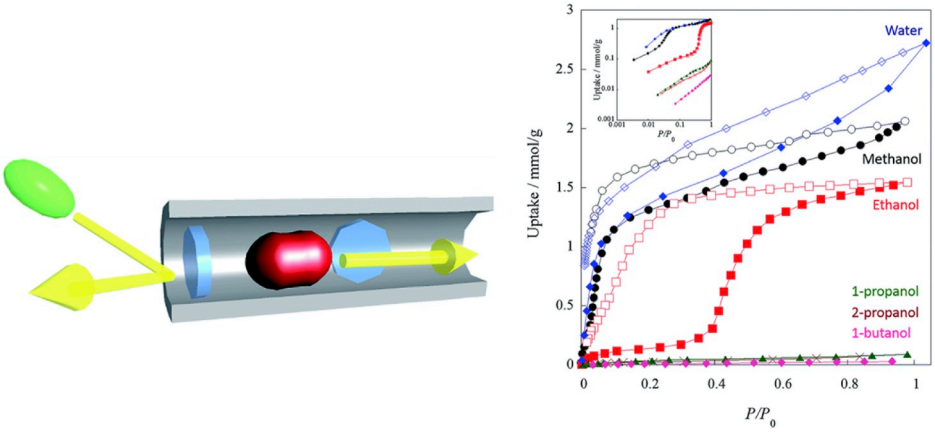

Fig. 14. Schematic illustration of the molecular gating of the 1D channel of $[Cu_2(tpt)_2(CH_3CN)_2](BF_4)_2$ (left). Blue plates correspond to the BF_4^- anions, red and green ellipsoids correspond to the adsorbate molecules accepted or unaccepted by the BF_4^- molecular gate. Water, methanol, ethanol, 1-propanol, 2-propanol and 1-butanol adsorption isotherms measured at 303 K (right) [78]. Reprinted with permission from ref. 78. Copyright (2018) Royal Chemistry Society. (For interpretation of the references to colour in this figure legend, the reader is referred to the Web version of this article.)

minor amounts of water from alcohols or to separate small quantities of alcohols from water [20,80]. Hereunder, it will be discussed relevant examples of MMMs used for the dehydration of alcohols and removal of alcohols from aqueous solutions.

3.1. Dehydration of alcohols

Dehydration of alcohols is usually carried out by pervaporation using hydrophilic membranes [20]. Water molecules are preferentially adsorbed and diffuse efficiently through the hydrophilic membranes due to their high hydrophilicity and small molecular size as compared with the alcohol molecules [20]. Nevertheless, the increased plasticization of the polymeric membranes reduces the diffusion of water molecules. Incorporating MOF crystals leads to enhanced fractional free volume and therefore increases the diffusion of water molecules. Moreover, the pores of the MOFs also contribute to the diffusion processes. Some MOFs are also hydrophilic and they enhance significantly the performance of the hydrophilic membranes.

Polybenzimidazole and chitosan membranes are two examples of hydrophilic membranes used for the dehydration of alcohols [80]. ZIFs have attracted attention as fillers in preparing polybenzimidazole and chitosan based MMMs due to their superior thermal and chemical stability as well as their former application in gas adsorption, storage and separation [81]. ZIFs are hydrophobic and may favor the adsorption of alcohols in their pores, thus decreasing the separation efficiency of the MMMs. However, it remains unclear the exact extent to which hydrophobic MOFs influence the dehydration of alcohols [82]. ZIF-8 nanoparticles with average size smaller than 50 nm were incorporated in a polybenzimidazole matrix used for the dehydration of ethanol, isopropanol and butanol [82]. The permeability of the mixture, reflected by the flux value, increased by increasing the loading of ZIF-8 in MMMs (Table 1). This is due to the disruption of the polymer-polymer packing of pristine polymeric membrane due to the incorporation of ZIF-8 nanoparticles. Thus, the MMMs structure becomes less dense. The pores of ZIF-8 further provide pathways for molecules permeation [82]. However, a further increase in ZIF-8 loading leads to a lower water/-alcohol separation factor of the ZIF-8/polybenzimidazole membrane. This is due to the damage of the polymer phase integrity as well as the increased defects in the polymer phase (Table 1) [82]. Lin et al. [83] incorporated ZIF-7 into a chitosan matrix to obtain a ZIF-7/chitosan MMM. Increasing the loading of ZIF-7 in the polymer matrix from 0 to *ca.* 5 wt% increases the water/ethanol separation factor from 148 to 2812. This is because the Zn^{2+} ions of ZIF-71 can bind to the amino groups of the chitosan polymer, narrowing the pore size of the chitosan matrix [82]. The ZIF-7/chitosan MMM with narrowed pores favors the selective adsorption of water over ethanol. However, the narrowed pore size also decreased the mixture permeability from 602 to 322 g/m^{2}h (Table 1) [83].

Table 1
MOFs-based MMMs used for the dehydration of alcohols.

MOF and loading (wt%)	Feed composition (wt%/wt%)	Temperature (°C)	Total flux (g/m^{2}h)	Separation factor (water/alcohol)	Reference
ZIF-8, 0; 33.7; 58.7	EtOH/H_2O (85/15)	60	151; 106; 992	4; 25.4; 10	82
ZIF-8, 0; 33.7; 58.7	*iso*propanol/H_2O (85/15)	60	13; 103; 246	>5000; 1686; 310	82
ZIF-8, 0; 33.7; 58.7	butanol/H_2O (85/15)	60	11.6; 81; 226	>5000; 3417; 698	82
ZIF-7, 0; 2.5	EtOH/H_2O (90/10)	25	602; 1206	148; 538;	83
ZIF-7, 4; 5	EtOH/H_2O (90/10)	25	858, 322	992; 2812	83
MOF-801, 4.8	EtOH/H_2O (90/10)	40	1937	2156	84

MOF-801/chitosan [84] was selected for water-alcohol separations because it has a good water stability and its structure is retained after several cycles of water adsorption measurements [85]. The high hydrophilic character of MOF-801 is responsible for the selective water adsorption of MOF-801/chitosan from water-ethanol mixtures. Analyzing the fractional accessible volume (FAV), it was found that the available free volume for water diffusion in MOF-801 is 1.4 times higher than that required for ethanol diffusion. This is due to the MOF-801's highly interconnected microporosity [84]. An optimized flux of *ca.* 1937 g/m^{2}h and a water/ethanol separation factor of 2156 were obtained by loading of 4.8 wt% of MOF-801 in a chitosan membrane (Table 1) [84].

3.2. Removal of alcohols from water-alcohol mixtures

A separate category of MOFs-based MMMs was designed for removing alcohols from water-alcohol mixtures by employing polymer matrixes with hydrophobic features that may favor the adsorption and diffusion of alcohols from the mixture [79]. Moreover, using hydrophobic MOFs enhances the selective adsorption of alcohols from water-alcohol mixtures [20].

Yang et al. [86] prepared MMMs by doping ZIF-8 nanoparticles as fillers in a silicone rubber polymethylphenylsiloxane matrix. This material with 10 wt% ZIF-8 loading has an *iso*butanol/water separation factor of *ca.* 35 and a flux of about 6400 g/m^{2}h for the separation of *iso*butanol from an aqueous mixture with *ca.* 1 wt% isobutanol (Table 2) [86]. The separation factor and permeability of

Table 2
MOFs based MMMs used for the removal of alcohols from aqueous mixtures.

MOF and loading (wt%)	Feed composition (wt%/wt%)	Temperature (°C)	Total flux (g/m^{2}h)	Separation factor (alcohol/water)	Reference
ZIF-8, 10	*iso*butanol/H_2O (1/99)	80	6400	34.9	86
ZIF-71, 20	acetone/*n*-butanol/ethanol/H_2O (0.6/1.2/0.2/98)	37	520.2	15.5	87
ZIF-71, 30	methanol/H_2O (5/95)	50	~1000	8.0	88
ZIF-71, 20	EtOH/H_2O (5/95)	50	~950	9.9	88
ZIF-71, 20	*iso*propanol/H_2O (5/95)	50	~1300	13.6	88
ZIF-71, 30	*sec*-butanol/H_2O (5/95)	50	~1550	30.2	88
MAF-6, 7.5	EtOH/H_2O (5/95)	60	4446	5.6	89

ZIF-8/polymethylphenylsiloxane are greatly improved as compared with the polymethylphenylsiloxane membrane. It is mainly related to the hydrophobic nature of ZIF-8 which enables the preferential adsorption and diffusion of *iso*butanol molecules [86]. Another interesting adsorbent material is ZIF-71/polyether-block-amide MMM [87]. It contains 20 wt% ZIF-71 and has a total organic component/water separation factor of *ca.* 15.5 and a total flux of 520 g/m^{2}h in a ternary aqueous mixture consisting of *ca.* 0.6 wt% of acetone, 1.2 wt% of *n*-butanol and 0.2 wt% of ethanol [87]. The adsorption selectivity observed is attributed to the high hydrophobicity of ZIF-71 [87].

A ZIF-71/polydimethylsiloxane MMM was synthesized with the aim of separating a series of alcohols from their 5 wt% aqueous solutions, including methanol, ethanol, *iso*propanol (IPA) and *sec*-butanol [88]. Adsorption studies show that the alcohol/water separation factors increased by increasing the ZIF-71 loading up to *ca.* 40%. This trend was attributed to the presence of ZIF-71 which shows selective alcohol adsorption [88]. Thus, the separation factors reach maximum values equal to 8 (methanol/water), 10 (ethanol/water), 13.5 (*iso*propanol/-water) and 30 (*sec*-butanol/water), respectively (Table 2). However, the alcohol/water separation factors decreased with further increasing the ZIF-71 loading above 30 wt%. Higher ZIF-71 loadings cause the damaging of the polydimethylsiloxane matrix integrity [88]. A hydrophobic MOF, namely RHO-[Zn(eim)$_2$] (known as MAF-6, where Heim = 2-ethylimidazole) was incorporated into a hydrophobic poly (ether-block-amide) membrane to remove ethanol from an ethanol-water mixture containing 5 wt% ethanol [89]. The ethanol/-water separation factor and the total flux were both improved due to the combined hydrophobicity of MAF-6 and poly(ether-block-amide) matrix. A total flux of *ca.* 4445 g/m^{2}h and a separation factor of *ca.* 5.5 were determined for this MMM with a 7.5 wt% loading of MAF-6 [89].

4. Conclusion

The main goal of this account was to assess the potential application of MOFs and their composite in water-alcohol adsorptive separations. Therefore, the design and synthesis strategies approaches of these MOFs and their composites as well as their performance in water/alcohol separations were reviewed. This review covers all the MOFs studied for their potential in water-alcohol separation applications. The examples discussed show that several approaches have been used to design MOFs for water-alcohol separations, but the number of studies is still very low. Among the various strategies used, designing and synthesizing MOFs with appropriate pore geometries as well as MOFs with flexible network topologies remain the most explored approaches. Yet, these studies focus mostly on material design and analysis of single adsorption isotherms and therefore insight regarding the separation efficiency is lacking. Furthermore, the MOF's stability, especially in the presence of water, is often not addressed, although this is a key requirement for practical applications.

The industrial separation of water-alcohol mixtures is performed through pervaporation and vapor permeation processes and therefore a few MMMs have been synthesized and tested as potential candidates for such processes. So far, the results show that the separation factor is related to the type of MOF filler, the matrix used and the mechanism by which molecules permeate the membranes and it also depends on the MOF loading in the polymer matrix. Therefore, designing MMMs with high permeability, selectivity and stability is still a challenging task. Consequently, a few questions are still to be answered before designing MOFs and MOF composite materials for the effective separation of water and alcohols: How can one control the MOF structure to yield specific channel dimensions? Which factors govern the competitive sorption of different alcohols? Can MOF materials be indeed optimized for industrial water-alcohol separation processes? We believe that more in-depth studies are required in order to answer these questions. Such studies should focus on developing new synthesis strategy for both MOFs as well as MOF-based composites aimed at increasing overall stability of the porous adsorbents during multiple adsorption cycles. Synthesizing water stable MOFs with inner adsorption sites as well as appropriate size of the pores is needed to enhance the potential applicability of MOFs in water-alcohol separation processes. The water stability can be enhanced by constructing metal-carboxylate MOFs containing high-valence metal ions, metal-azolate MOFs with nitrogen-donor ligands or using MOFs with hydrophobic pore surfaces or containing blocked metal ions [90]. The inner adsorption sites can be tuned by modifying the surface properties of a MOF's framework. It can be achieved by either synthesizing MOFs starting from functionalized ligands bearing hydrophobic or hydrophilic organic groups or by post-synthetic modification using reactive centers on the MOF for grafting chemical functions [91]. The rational design of MOFs with appropriate pore size to distinguish water and alcohol molecules is still very challenging and it requires in-depth studies. Developing new synthetic approaches may bring further insight in the design principles of selective adsorbent materials for water-alcohol separations. applications [92]. A recent study reported the design of a novel adsorbent material obtained by growing ZIF-8 crystals at the surface of mixed-oxide support with a hierarchical porous structure [93]. The approach developed provided not only a new methodology for the processing MOFs as composites but also led to improved separation of water-alcohol and alcohol-alcohol mixtures [93]. It was also shown that introducing organic polymers within the 1D pores of DMOF enables to fine tune the pore's size of adsorbent materials [94]. Specific organic polymers can undergo a phase transition between hydrophobic and hydrophilic phases in response to a low temperature change. This property can be used to control the desorption of water and alcohol molecules, therefore enabling an efficient and cost effective regeneration process [94].

Declaration of competing interest

The authors declare that they have no known competing financial interests or personal relationships that could have appeared to influence the work reported in this paper.

Acknowledgements

YT acknowledges the China Scholarship Council (CSC) for a PhD fellowship. This work is part of the Research Priority Area Sustainable Chemistry of the University of Amsterdam, http://suschem.uva.nl.

References

[1] S.I. Mussatto, G. Dragone, P.M.R. Guimarães, J.P.A. Silva, L.M. Carneiro, I. C. Roberto, A. Vicente, L. Domingues, J.A. Teixeira, Biotechnol. Adv. 28 (2010) 817–830.
[2] J. Baeyens, Q. Kang, L. Appels, R. Dewil, Y. Lv, T. Tan, Prog. Energy Combust. Sci. 47 (2015) 60–88.
[3] S. Kim, B.E. Dale, Biomass Bioenergy 26 (2004) 361–375.
[4] D. Luo, Z. Hu, D.G. Choi, V.M. Thomas, M.J. Realff, R.R. Chance, Environ. Sci. Technol. 44 (2010) 8670–8677.
[5] K.P. Moller, W. Bohringer, A.E. Schnitzler, E. van Steen, C.T. O'Connor, Microporous Mesoporous Mater. 29 (1999) 127–144.
[6] B. Elvers, Handbook of Fuels, Wiley-WCH, Weinheim, 2008.
[7] K. Zhang, R.P. Lively, C. Zhang, W.J. Koros, R.R. Chance, J. Phys. Chem. C 117 (2013) 7214–7225.
[8] B.V. de Voorde, B. Bueken, J. Denayer, D.D. Vos, Chem. Soc. Rev. 43 (2014) 5766–5788.
[9] K. Okamoto, H. Kita, K. Horii, K. Tanaka, Ind. Eng. Chem. Res. 40 (2001) 163–175.
[10] V.A. Tuan, S. Li, J.L. Falconer, R.D. Noble, J. Memb. Sci. 196 (2002) 111–123.
[11] R.K. Motkuri, P.K. Thallapally, H.V. Annapureddy, L.X. Dang, R. Krishna, S. K. Nune, C.A. Fernandez, J. Liu, B.P. McGrail, Chem. Commun. 51 (2015) 8421–8424.
[12] H.B. Aditiya, T.M.I. Mahlia, W.T. Chong, H. Nur, A.H. Sebayang, Renew. Sustain. Energy Rev. 66 (2016) 631–653.
[13] S. Kumar, N. Singh, R. Prasad, Renew. Sustain. Energy Rev. 14 (2010) 1830–1844.
[14] J.-R. Li, R.J. Kuppler, H.-C. Zhou, Chem. Soc. Rev. 38 (2009) 1477–1504.
[15] G. Rutkai, É. Csányi, T. Kristóf, Microporous Mesoporous Mater. 114 (2008) 455–464.
[16] N. Qureshi, S. Hughes, I.S. Maddox, M.A. Cotta, Bioproc. Biosyst. Eng. 27 (2005) 215–222.
[17] V. Smuleac, J. Wu, S. Nemser, S. Majumdar, D. Bhattacharyya, J. Memb. Sci. 352 (2010) 41–49.
[18] L.M. Vane, Biofuels Bioprod. Bioref. 2 (2008) 553.
[19] T.C. Bowen, L.M. Vane, Langmuir 22 (2006) 3721–3727.
[20] Z. Jia, G. Wu, Microporous Mesoporous Mater. 235 (2016) 151–159.
[21] H.-C. Zhou, S. Kitagawa, Chem. Soc. Rev. 43 (2014) 5415–5418.
[22] M. Eddaoudi, J. Kim, N. Rosi, D. Vodak, J. Wachter, M. O'Keeffe, O.M. Yaghi, Science 295 (2002) 469–472.
[23] X. Xuan, C. Zhu, Y. Liu, Y. Cui, Chem. Soc. Rev. 41 (2012) 1677–1695.
[24] R. Krishna, J.R. Long, J. Phys. Chem. C 115 (2011) 12941–12950.
[25] Z. Wang, S.M. Cohen, Chem. Soc. Rev. 38 (2009) 1315–1329.
[26] D. Zhao, D.J. Timmons, D. Yuan, H.-C. Zhou, Acc. Chem. Res. 44 (2011) 123–133.
[27] F.A. Almeida Paz, J. Klinowski, S.M.F. Vilela, J.P.C. Tomé, J.A.S. Cavaleiro, J. Rocha, Chem. Soc. Rev. 41 (2012) 1088–1110.
[28] Y. Bai, Y. Dou, L.-H. Xie, W. Rutledge, J.-R. Li, H.-C. Zhou, Chem. Soc. Rev. 45 (2016) 2327–2367.
[29] K.M. Fromm, Coord. Chem. Rev. 252 (2008) 856–885.
[30] J. Yu, L.-H. Xie, J.-R. Li, Y. Ma, J.M. Seminario, P.B. Balbuena, Chem. Rev. 117 (2017) 9674–9754.
[31] J. Liu, Y. Wei, Y. Zhao, ACS Sustain. Chem. Eng. 7 (2019) 82–93.
[32] D.-X. Xue, Q. Wang, J. Bai, Coord. Chem. Rev. 378 (2019) 2–16.
[33] H.W. Langmi, J. Ren, B. North, M. Mathe, D. Bessarabov, Electrochim. Acta 128 (2014) 368–392.
[34] Y. Lin, C. Kong, Q. Zhang, L. Chen, Adv. Energy Mater. 7 (2017) 1601296.
[35] M. Gehre, Z. Guo, G. Rothenberg, S. Tanase, ChemSusChem 10 (2017) 3947–3963.
[36] Z.R. Herm, E.D. Bloch, J.R. Long, Chem. Mater. 26 (2014) 323–338.
[37] X. Zhang, X. Lv, X. Shi, Y. Yang, Y. Yang, J. Colloid Interface Sci. 539 (2019) 152–160.
[38] X. Zhang, Y. Yang, X. Lv, Y. Wang, N. Liu, D. Chen, L. Cui, J. Hazard Mater. 366 (2019) 140–150.
[39] X. Zhang, Y. Yang, L. Song, J. Chen, Y. Yang, Y. Wang, J. Hazard Mater. 365 (2019) 597–605.
[40] M.F. de Lange, B.L. van Velzen, C.P. Ottevanger, K.J.F.M. Verouden, L.-C. Lin, T.J. H. Vlugt, J. Gascon, F. Kapteijn, Langmuir 31 (2015) 12783–12796.
[41] R. Plenderleith, T. Swift, S. Rimmer, RSC Adv. 4 (2014) 50932–50937.
[42] K.J. Gagnon, H.P. Perry, A. Clearfield, Chem. Rev. 112 (2012) 1034–1054.
[43] Z.-J. Lin, J. Lü, M. Hong, R. Cao, Chem. Soc. Rev. 43 (2014) 5867–5895.
[44] T.-F. Liu, J. Lü, X. Lin, R. Cao, Chem. Commun. 46 (2010) 8439–8441.
[45] A. Nalaparaju, X.S. Zhao, J.W. Jiang, J. Phys. Chem. C 114 (2010) 11542–11550.
[46] A. Shigematsu, T. Yamada, H. Kitagawa, J. Am. Chem. Soc. 134 (2012) 13145–13147.
[47] D. Tanaka, K. Nakagawa, M. Higuchi, S. Horike, Y. Kubota, T.C. Kobayashi, M. Takata, S. Kitagawa, Angew. Chem. Int. Ed. 47 (2008) 3914–3918.
[48] P.D. Smith, B.R. James, D.H. Dolphin, Coord. Chem. Rev. 39 (1981) 31–75.
[49] N.C. Burtch, S. Walton, Acc. Chem. Res. 48 (2015) 2850–2857.
[50] P.K. Thallapally, J. Tian, M.R. Kishan, C.A. Fernandez, S.J. Dalgarno, P.B. McGrail, J.E. Warren, L. Atwood, J. Am. Chem. Soc. 130 (2008) 16842–16843.
[51] C. Hou, Y.-L. Bai, X. Bao, L. Xu, R.-G. Lin, S. Zhu, J. Fang, J. Xu, Dalton Trans. 44 (2015) 7770–7773.
[52] G. Férey, C. Serre, Chem. Soc. Rev. 38 (2009) 1380–1399.
[53] S. Sanda, S. Parshamoni, S. Konar, Inorg. Chem. 52 (2013) 12866–12868.
[54] E.R. Engel, A. Jouaiti, C.X. Bezuidenhout, M.W. Hosseini, L.J. Barbour, Angew. Chem. Int. Ed. 56 (2017) 8874–8878.
[55] S. Bourrelly, B. Moulin, A. Rivera, G. Maurin, S. Devautour-Vinot, C. Serre, T. Devic, P. Horcajada, A. Vimont, G. Clet, M. Daturi, J.-C. Lavalley, S. Loera-Serna, R. Denoyel, P.L. Llewellyn, G. Férey, J. Am. Chem. Soc. 132 (2010) 9488–9498.
[56] C. Serre, F. Millange, C. Thouvenot, M. Noguè, G. Marsolier, D. Louër, G. Férey, J. Am. Chem. Soc. 124 (2002) 13519–13526.
[57] J.Y. Lee, D.H. Olson, L. Pan, T.J. Emge, J. Li, Adv. Funct. Mater. 17 (2007) 1255–1262.
[58] Y.F. Chen, J.Y. Lee, R. Babarao, J. Li, J.W. Jiang, J. Phys. Chem. C 114 (2010) 6602–6609.
[59] K. Zhang, R.P. Lively, M.E. Dose, A.J. Brown, C. Zhang, J. Chung, S. Nair, W. J. Koros, R.R. Chance, Chem. Commun. 49 (2013) 3245–3247.
[60] R.P. Lively, M.E. Dose, J.A. Thompson, B.A. McCool, R.R. Chance, W.J. Koros, Chem. Commun. 47 (2011) 8667–8669.
[61] D.N. Dybtsev, H. Chun, K. Kim, Angew. Chem. Int. Ed. 116 (2004) 5033–5036.
[62] G.F. de Lima, A. Mavrandonakis, H.A. De Abreu, H.A. Duarte, T. Heine, J. Phys. Chem. C 117 (2013) 4124–4130.
[63] P.M. Schoenecker, C.G. Carson, H. Jasuja, C.J.J. Flemming, K.S. Walton, Ind. Eng. Chem. Res. 51 (2012) 6513–6519.
[64] H. Jasuja, N.C. Burtch, Y.-G. Huang, Y. Cai, K.S. Walton, Langmuir 29 (2013) 633–642.
[65] B.R. Pimentel, A. Parulkar, E.-K. Zhou, N.A. Brunelli, R.P. Lively, ChemSusChem 7 (2014) 3202–3240.
[66] A. Nalaparaju, X.S. Zhao, J.W. Jiang, J. Phys. Chem. C 114 (2010) 11542–11550.
[67] J.-K. Sun, M. Ji, C. Chen, W.-G. Wang, P. Wang, R.-P. Chen, J. Zhang, Chem. Commun. 49 (2013) 1624–1626.
[68] B. Chen, Y. Ji, M. Xue, F.R. Fronczek, E.J. Hurtado, J.U. Mondal, C. Liang, S. Dai, Inorg. Chem. 47 (2008) 5543–5545.
[69] K. Li, D.H. Olson, J.Y. Lee, W. Bi, K. Wu, T. Yuen, Q. Xu, J. Li, Adv. Funct. Mater. 18 (2008) 2205–2214.
[70] T. Borjigin, F. Sun, J. Zhang, K. Cai, H. Ren, G. Zhu, Chem. Commun. 48 (2012) 7613–7615.
[71] X. Zheng, Y. Huang, J. Duan, C. Wang, L. Wen, J. Zhao, D. Li, Dalton Trans. 43 (2014) 8311–8317.
[72] Y. Huang, X. Zheng, J. Duan, W. Liu, L. Zhou, C. Wang, L. Wen, J. Zhao, D. Li, Dalton Trans. 43 (2014) 6811–6818.
[73] R. Plessius, R. Kromhout, A.L.D. Ramos, M. Ferbinteanu, M.C. Mittelmeijer-Hazeleger, R. Krishna, G. Rothenberg, S. Tanase, Chem. Eur J. 20 (2014) 7922–7925.
[74] P. Ju, L. Jiang, T.-B. Lu, Inorg. Chem. 54 (2015) 6291–6295.
[75] J. Duan, W. Jin, S. Kitagawa, Coord. Chem. Rev. 332 (2017) 48–74.
[76] N.C. Burtch, H. Jasuja, K.S. Walton, Chem. Rev. 114 (2014) 10575–10612.
[77] Y. Sha, S. Bai, J. Lou, D. Wu, B. Liu, Y. Ling, Dalton Trans. 45 (2016) 7235–7239.
[78] A. Kondo, T. Yashiro, N. Okada, S. Hiraide, T. Ohkubo, H. Tanaka, K. Maeda, J. Mater. Chem. A 6 (2018) 5910–5918.
[79] J. Ren, N.M. Musyokam, H.W. Langmi, A. Swartbooi, B.C. North, M.A. Mathe, Int. J. Hydrogen Energy 40 (2015) 4617–4622.
[80] P. Shao, R.Y.M. Huang, J. Membr. Sci. 287 (2007) 162–179.
[81] V.M.A. Melgar, J. Kim, M.R. Othman, J. Ind. Eng. Chem. 28 (2015) 1–15.
[82] G.M. Shi, T. Yang, T.S. Chung, J. Membr. Sci. 577 (2012) 415–416.
[83] C.-H. Kang, Y.-F. Lin, Y.-S. Huang, K.-L. Tung, K.-S. Chang, J.-T. Chen, W.-S. Hung, K.-R. Lee, J.-Y. Lai, J. Membr. Sci. 438 (2013) 105–111.
[84] Q. Li, Q. Liu, J. Zhao, Y. Hua, J. Sun, J. Duan, W. Jin, J. Membr. Sci. 544 (2017) 68–78.
[85] H. Furukawa, F. Gandara, Y.-B. Zhang, J. Jiang, W.L. Queen, M.R. Hudson, O. M. Yaghi, J. Am. Chem. Soc. 136 (2014) 4369–4381.
[86] X.-L. Liu, Y.-S. Li, G.-Q. Zhu, Y.-J. Ban, Y.-Y. Xu, W.-S. Yang, Angew. Chem. Int. Ed. 123 (2011) 10824.
[87] S. Liu, G. Liu, X. Zhao, W. Jin, J. Membr. Sci. 446 (2013) 181–188.
[88] Y. Li, L.H. Wee, J.A. Martens, I.F.J. Vankelecom, J. Mater. Chem. A 2 (2014) 10034–10040.
[89] Q. Liu, Y. Li, Q. Li, G. Liu, G. Liu, W. Jin, Separ. Purif. Technol. 214 (2019) 2–10.
[90] C. Wang, X. Liu, N.K. Demir, J.P. Chen, K. Li, Chem. Soc. Rev. 45 (2016) 5107–5134.
[91] J. Canivet, A. Fateeva, Y. Guo, B. Coasne, D. Farrusseng, Chem. Soc. Rev. 43 (2014) 5594–5617.
[92] M.-H. Sun, S.-Z. Huang, L.-H. Chen, Y. Li, X.-Y. Yang, Z.-Y. Yuan, B.-L. Su, Chem. Soc. Rev. 45 (2016) 3479–3563.
[93] Y. Tang, D. Dubbeldam, X. Guo, G. Rothenberg, S. Tanase, ACS Appl. Mater. Interfaces 11 (2019) 21126–21136.
[94] Y. Tang, D. Dubbeldam, S. Tanase, ACS Appl. Mater. Interfaces 11 (2019), https://doi.org/10.1021/acsami.9b14367.